geomatics

MDPI

Article

Characterizing Alboran Sea Frontal Dynamics: A Multi-Variable Analysis with GRADHIST in Data Cubes

Elena Martínez-Mateo [1,*] and Ana B. Ruescas [1,2,*]

[1] Image Processing Laboratory, University of València, Parc Científic, C/ Cat. Agustín Escardino Benlloch, 9, Paterna, 46980 València, Spain
[2] Department of Geography, University of València, Avda. Blasco Ibañez, 28, 46010 València, Spain
* Correspondence: emarma5@alumni.uv.es (E.M.-M.); ana.b.ruescas@uv.es (A.B.R.)

Abstract

In this study, we used the DeepESDL framework to exploit multivariate data cubes for the identification and characterization of frontal zones in the Alboran Sea throughout the year 2023. By operating directly within a unified data hypercube architecture, we seamlessly evaluate the spatial coherence and temporal evolution across highly disparate environmental variables. We adapted the Gradient Histogram Method (GRADHIST) algorithm to run efficiently on data cube tracks of sea surface temperature (SST), sea surface height (SSH), sea surface salinity (SSS), and chlorophyll-a concentration (CHL) fields. This multi-dimensional approach enabled a detailed, synchronized description of the spatial distribution and evolution of fronts. The GRADHIST algorithm proved highly adaptable to the data cube format, utilizing a dynamic threshold that optimizes front detection across fields of fundamentally different physical natures and dynamic ranges.

Keywords: marine fronts; GRADHIST; remote sensing; data-cubes

1. Introduction

The study of oceanic processes on the submesoscale (1 to 10 km) has gained increasing relevance in recent decades due to their essential role in marine dynamics, biological connectivity, and the transport of physical and bio-geochemical properties [1]. Structures—such as filaments, eddies, and fronts—act as drivers of vertical mixing, redistribute heat and nutrients, and can enhance biological productivity. The development of high temporal resolution satellite observation platforms—such as Sentinel 3 sensors (OLCI, SLSTR) and derived products from the Copernicus Marine Environment Monitoring Service (CMEMS)—has enabled the study of these processes with unprecedented detail, bringing remote sensing closer to submesoscale dynamics [2,3].

Within the Mediterranean Sea, the Alboran Sea represents one of the most dynamic and complex oceanographic environments. Located between the Strait of Gibraltar and the Almeria Sea, it functions as a transition zone between incoming Atlantic waters (colder and less saline) and Mediterranean waters (warmer and more saline). The interaction between these contrasting water masses generates a variety of oceanic structures, increasing the value of the region as an area of high oceanographic significance. Among these structures there are semi-permanent eddies, such as the Western and Eastern Alboran Gyres, and coastal jets and well-defined fronts, such as the Almeria-Oran front-one of the most persistent and extensively studied structures in the region [4,5]. The Alborean Region is of great natural importance for the study of submesoscale processes and their bio-geochemical

Check for updates

Academic Editor: Gabriel Navarro

Received: 30 June 2026
Revised: 8 August 2026
Accepted: 17 August 2026
Published: 25 August 2026

Copyright: © 2026 by the authors. Licensee MDPI, Basel, Switzerland. This article is an open access article distributed under the terms and conditions of the Creative Commons Attribution (CC BY) license.

implications due to its high spatio-temporal variability, its complex topography and its role as a transition zone between contrasting water masses [6,7]. Focusing on frontal zones, these regions are characterized by intense gradients in variables such as sea surface temperature (SST), sea surface salinity (SSS), sea surface height (SSH) and chlorophyll-a concentration (CHL). These variables allow for the delineation of boundaries between water masses with contrasting properties and are key to understanding characteristic oceanic processes in the region, such as coastal upwelling, vertical mixing, and biological distribution [8]. Furthermore, frontal zones often coincide with biodiversity hotspots and areas of high primary productivity, making them ecologically and socioeconomically important due to their association with major fishing grounds [9,10]. Nevertheless, accurate detection of these structures is challenging, as satellite data can present spatial gaps, noise, or insufficient resolution, limiting the reliable identification of fronts [11]. During the past decade, automated front detection using satellite observations has become a key tool for habitat monitoring, ecosystem modeling, and marine resource management [12].

From a review of the existing literature related to the use of satellite data in the Alboran Sea, we can observe that spatial resolution is an important factor for understanding ocean circulation and detecting frontal structures, particularly in coastal areas [13]. This aspect is especially relevant for the identification of localized frontal structures, as they may appear smoothed or be insufficiently represented when lower spatial resolutions are used.

In response to these limitations, there is a growing need for objective and computationally efficient methods capable of characterizing spatial variability in large datasets in a reproducible manner. Such techniques enable near-real-time identification of zones of physical and ecological convergence, improving the understanding of physical–biological coupling. In this context, the GRADHIST algorithm [14] represents a particularly suitable tool for oceanic front detection. Its principle is based on computing the magnitude of the horizontal gradient of a marine variable (e.g., SST or CHL), followed by the construction of a frequency histogram that describes the statistical distribution of these gradients. The use of statistical thresholds, such as the 90th or 95th percentile, allows the identification of regions with high spatial variability, typically associated with fronts or discontinuities [8]. Compared to more complex approaches, GRADHIST is objective, straightforward to implement, and computationally efficient, making it well suited for high-resolution regional studies. Another key aspect of this method is its proven effectiveness in detecting fronts based on temperature and chlorophyll gradients across various oceanic regions, including the North Atlantic and the tropical Pacific [8,14], supporting its applicability to high-resolution regional studies.

Based on the above considerations, the GRADHIST algorithm is applied to high-resolution (4 km) daily multi-variable datasets obtained from the Copernicus Marine Environment Monitoring Service (CMEMS) (https://marine.copernicus.eu, accessed on 20 June 2026), and processed using XCUBE tools (https://xcube.readthedocs.io/en/latest/, accessed on 20 June 2026) platform from the European Space Agency. Four fundamental variables are analyzed—SST, SSS, SSH, and CHL—all of which are relevant to describe physical and bio-geochemical ocean processes. The main objective is to detect and characterize frontal zones in the Alboran Sea, evaluating their spatial coherence across variables and their temporal evolution throughout the year 2023. This work aims to contribute to a better understanding of Mediterranean submesoscale dynamics and to the development of reproducible methodologies for front detection using satellite data. The results are expected to improve the characterization of frontal dynamics and provide a foundation for future applications in operational monitoring and ecosystem modeling.

2. Datasets and Study Region

We rely on high temporal resolution oceanographic data obtained through the Copernicus Marine Environment Monitoring Service (CMEMS) and integrated through the Deep Earth System Data Lab (DeepESDL) platform, building a hypercube with the XCUBE tool for data management and subsequent analysis. CMEMS is a European service responsible for providing open-access global and regional ocean observations and analyses. The available products combine satellite data, in situ observations, and validated numerical models, ensuring temporal and spatial consistency. In our study area, CMEMS products are generated by Mercator Ocean International and CNR-GOS (Consiglio Nazionale delle Ricerche—Group for Ocean Satellite data), with a particular emphasis on monitoring marine physics and biogeochemistry [15,16]. DeepESDL is an infrastructure designed for the efficient access to and analysis of large volumes of geophysical data. It enables the manipulation of multidimensional data cubes (space–time–variable) through an interactive environment. Within this platform, the XCUBE tool provides a data structure compatible with xarray and Dask, thereby facilitating distributed processing and interoperability between different satellite and model-based data sources.

2.1. Selected Variables and Datasets

For this analysis, four key variables were considered for characterizing the surface dynamics of the Alboran Sea: sea surface temperature (SST), sea surface salinity (SSS), sea surface height (SSH), and chlorophyll-a concentration (CHL). All variables were selected for the period from 1 January to 31 December 2023, covering a spatial domain encompassing the Alboran Sea.

Each selected variable provides complementary information on physical and biogeochemical processes at the sea surface:

- SST represents the surface thermal distribution and allows the identification of fronts and eddies through horizontal thermal gradients, which are indicators of mixing or convergence of water masses.
- SSH reflects the dynamic structure of the surface pressure field and is associated with geostrophic circulation. Local variations in SSH allow the inference of cyclonic and anticyclonic gyres characteristic of the Alboran Sea.
- SSS acts as a tracer of water masses and their mixing, being particularly relevant in this region where Atlantic waters (colder and less saline) and Mediterranean waters (warmer and more saline) converge.
- CHL is an indicator of phytoplankton biomass and primary productivity. Its surface distribution is strongly modulated by physical processes such as upwelling, convergence, and fronts, thus complementing the physical interpretation.

The combined analysis of these variables allows linking physical patterns (SST, SSH, SSS) with the biological response (CHL), facilitating the identification of zones of interaction between dynamic and bio-geochemical processes. The physical variables (SST, SSS, and SSH) are extracted from the CMEMS regional physical model MED_PHY, corresponding to the product `cmems_mod_med_phy_anfc_4.2km_P1D-m`, with a spatial resolution of 4.2 km and daily frequency. This model is based on a data assimilation scheme that combines satellite observations and in situ profiles, providing a consistent representation of the circulation and thermal structure of the Mediterranean Sea. The chlorophyll-a variable is obtained from the bio-geochemical product `cmems_obs-oc_med_bgc-plankton_my_4-gapfree-multi-1km_P1D`, generated by CNR-GOS using multi-sensor ocean color observations (MODIS, VIIRS, and OLCI) (Table 1). This product internally applies reconstruction techniques based on empirical orthogonal functions (EOFs) to provide continuous daily coverage; however, in this study, the data

were used directly as preprocessed, without applying additional reconstructions or interpolation techniques.

Table 1. Datasets used in this study.

Var.	Unit	Product	Resolution	Frequency
SST	°C	CMEMS MED_PHY	4.2 km	Daily
SSH	m	CMEMS MED_PHY	4.2 km	Daily
SSS	PSU	CMEMS MED_PHY	4.2 km	Daily
CHL	mg m^{-3}	CMEMS MED_BGC	1 km	Daily

Since the different variables had different spatial resolutions, it was necessary to unify the resolution for a comprehensive joint analysis. The analyzed period covers the entire year 2023, selected because it provides complete and consistent coverage among the different CMEMS products, with no temporal gaps or discontinuities. This year is considered representative of the recent climatology of the western Mediterranean, without extreme events that could significantly alter the circulation of the Alboran Sea. Therefore, the selected products provide a coherent, high-resolution multi-variable description of the area. Integration through DeepESDL and the use of the XCUBE format enabled efficient handling of large data volumes, ensuring the reproducibility of the analysis.

2.2. Study Site

The study area corresponds to the Alboran Sea, located in the westernmost Mediterranean basin between approximately 33° N–39° N and 5° W–5° E (Figure 1). This region represents a key transition zone between the Atlantic Ocean and the Mediterranean Sea, where relatively fresh and colder Atlantic waters enter through the Strait of Gibraltar and interact with warmer and saltier Mediterranean waters, generating strong horizontal gradients and intense dynamical activity [17,18].

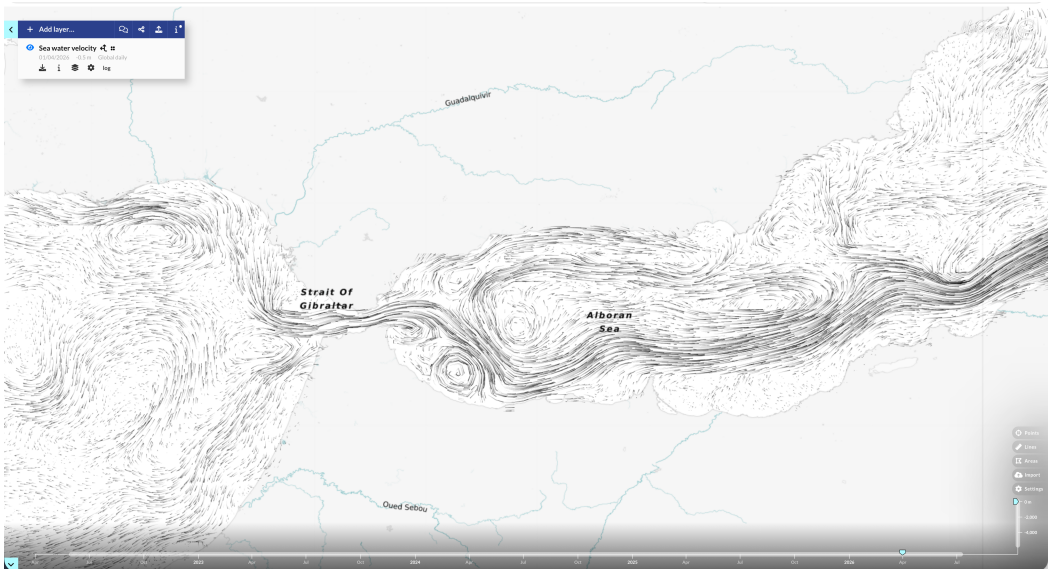


Figure 1. Study area showing the Alboran Sea domain and main circulation features in April. Source: MyOceanPro, CMEMS.

The surface circulation of the Alboran Sea is dominated by salinity changes. The Atlantic Water (AW) suffers a change in salinity in its way to the Mediterranean basin due to the influx of the Levantine Intermediate Water (LIW, 200–600 m depth), and stays closer to the surface (50–150 m depth). The Mediterranean Deep Water (MDW), with lower salinity

and temperature stays below the AW and the LIW. The AW flows eastward after entering through the Strait of Gibraltar and gives rise to two semi-permanent anticyclonic gyres: the Western Alboran Gyre (WAG) and the Eastern Alboran Gyre (EAG). These structures play a fundamental role in the redistribution of water masses and in the generation of mesoscale variability [19,20]. The interaction between the Atlantic inflow and the resident Mediterranean waters leads to the formation of the Almeria–Oran Front, a quasi-permanent feature that separates distinct water masses and constitutes one of the most prominent dynamical structures in the region [21].

These circulation patterns promote the development of mesoscale and submesoscale features, including fronts, filaments, and eddies, which are characterized by strong gradients in SST, SSS, SSH, and CHL concentration. Such structures play a key role in modulating vertical exchanges, lateral transport, and biogeochemical processes, often enhancing primary productivity and leading to the accumulation of phytoplankton biomass in frontal regions [1]. The coupling between physical dynamics and biological response is therefore particularly relevant in this region, making the Alboran Sea an ideal natural laboratory for studying submesoscale processes.

In addition to basin-scale circulation, coastal processes such as upwelling along the northern African margin and parts of the Iberian coast contribute to localized increases in nutrient availability and biological productivity [22]. However, these processes typically occur at spatial scales smaller than the resolution of the datasets used in this study (4.2 km for physical variables), which may limit their accurate representation and lead to a partial smoothing of coastal gradients.

Frontal structures generally occupy a relatively small fraction of the total study domain, on the order of approximately 10% of the surface area, while the majority of the basin is characterized by relatively weak gradients. As a consequence, statistical metrics computed over the entire domain may be significantly influenced by non-frontal regions, leading to an underestimation of the intensity and variability associated with frontal dynamics. Therefore, the results presented in this study should be interpreted as basin-scale averages rather than as values representative exclusively of frontal zones.

3. Methodology

The work carried out in this study was divided into four phases: (1) acquisition and pre-processing of multi-variable satellite data; (2) construction of homogeneous data cubes in space and time and the compilation of the hypercube (see Section 3.1); (3) computation of spatial gradients using the GRADHIST algorithm (Section 3.2); and (4) statistical analysis and visualization of the detected frontal zones (see Section 4).

3.1. Acquisition, Construction and Pre-Processing of Data Cubes

The work was performed using the DeepESDL platform, supported by ESA, an environment that enables the manipulation and advanced analysis of multidimensional data through the XCUBE library. The XCUBE tool, facilitates the generation of data cubes that are homogeneous in space, time and resolution, which is essential for the joint study of different oceanographic variables. Each variable data (SST, SSS, SSH and CHL) was downloaded using Application Programming Interfaces (APIs), delimiting a spatial domain between 34° N and 38° N, and 5° W and 5° E, encompassing the entire Alboran Sea and its immediate surroundings. Subsequently, the datasets were transformed into three-dimensional data cubes with coordinates (time, latitude, longitude), removing any additional vertical dimension, such as depth, which was not relevant for this surface analysis. To ensure spatial consistency among the different products, all data cubes were interpolated to a uniform resolution of 4 km using bilinear interpolation. Bilinear interpolation may

introduce a degree of spatial smoothing, particularly for the original 1 km CHL product when resampled to 4 km (Figure 2). Consequently, small-scale variability and sharp frontal gradients may be partially smoothed, potentially resulting in lower gradient magnitudes than those obtained at the original spatial resolution. This effect is considered a limitation of the common-resolution approach adopted to ensure spatial consistency among the four variables. This resolution was selected as a compromise between the ability to detect submesoscale structures (1–10 km) and the need to maintain compatibility among products derived from different sources (physical models and satellite observations). Once the consistency of dimensions and temporal coordinates (365 daily time steps for 2023) was verified, the four cubes were integrated into a single multi-variable dataset or hypercube, forming the analytical basis of the study. The analysis was performed using the original daily observations for 2023, without applying temporal moving-average smoothing.

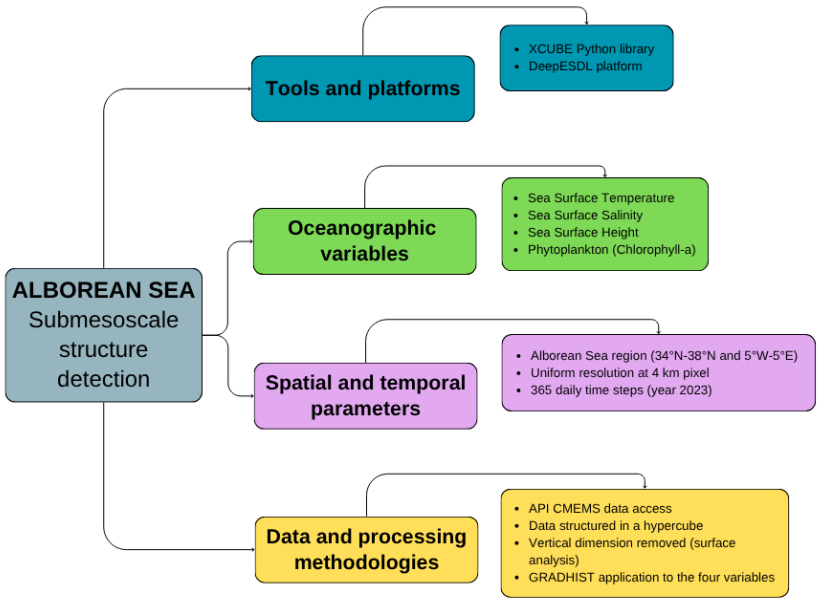


Figure 2. Summary of the data and methodology.

3.2. Gradient Computation and Front Detection Using the GRADHIST Algorithm

The detection of frontal structures was performed by applying the Gradient Histogram Method (GRADHIST) algorithm [14], originally developed for the analysis of high-resolution satellite-derived sea surface temperature fields. In its original formulation, the method exploits the statistical properties of horizontal gradients to identify oceanic fronts, assuming that frontal regions are associated with the high-gradient tail of the probability distribution. With this approach areas of high variability are indicative of dynamic fronts. The GRADHIST approach takes advantage of gradients algorithms to detect fronts plus the histogram algorithms, which work with the frequency distribution of the values within one image. It combines and modifies the gradient algorithm of Canny (1986) [23] and the histogram algorithm of Cayula and Cornillon (1992) [24] improving the front detection. For more details on the basis and implementation with MERIS data see [14]. GRADHIST is able of detection of strong and weak fronts, the determination of the gradient magnitude as well as the gradient direction.

After the application of the GRADHIST approach and the computation of the gradient magnitude and gradient direction, the statistical analysis is done as follows: For each time step, the zonal and meridional derivatives of each variable $(\partial X/\partial x, \partial X/\partial y)$ are calculated from the spatial differences between adjacent grid cells in the longitudinal and latitudinal directions. To avoid numerical biases and scale discrepancies, horizontal distances are

converted to meters taking into account the curvature of the Earth. These derivatives are combined to obtain the mean of the magnitude of the horizontal gradient Equation (1):

$$|\nabla V| = \sqrt{\left(\frac{\partial V}{\partial x}\right)^2 + \left(\frac{\partial V}{\partial y}\right)^2} \quad (1)$$

where V represents any of the analyzed oceanographic variables (SST, SSS, SSH, or CHL). The resulting $|\nabla V|$ indicates the intensity of the spatial change of V, with higher values corresponding to areas of strong variability, typically associated with oceanic fronts.

The computation is implemented iteratively for each day of the year, thereby generating a three-dimensional field of gradient magnitudes $|\nabla X|(t, \text{lat}, \text{lon})$. Once the gradients are obtained, a frequency histogram of the $|\nabla X|$ magnitudes is constructed. This distribution typically exhibits a skewed shape toward higher values, characteristic of frontal regions. Following the original methodology of [14] a dynamic threshold corresponding to the 90th percentile of the distribution is defined. Pixels with values exceeding this threshold are classified as frontal zones, enabling an objective delineation of the most active structures.

In this work we have extended the original GRADHIST methodology by moving from a single-variable (SST-only) framework to a multi-variable formulation including SST, SSS, SSH, and CHL. This extension allows a more comprehensive representation of coupled physical and biogeochemical fronts, and enhances the capability to capture submesoscale variability in dynamically active regions such as the Alboran Sea.

4. Results

Using the daily gradient fields and the derived frontal masks, temporal variations in frontal intensity are analyzed throughout the year. Multitemporal composites are generated to visualize the seasonal evolution and displacement of dominant fronts, particularly around the Western and Eastern Alboran Gyres and the Almeria–Oran Front. The analysis is complemented with descriptive statistics of frontal extent and persistence, quantifying the relative frequency of occurrence of active regions over the study period. This information allows the identification of areas with higher recurrence of submesoscale activity, as well as potential relationships with seasonal dynamics or external forcings (winds, Atlantic inflow, density gradients).

Temporal Analysis and Visualization of Frontal Variability

The application of the GRADHIST method to the hypercube (SST, SSH, SSS, and CHL) for the period from 1 January to 31 December 2023 allowed the objective identification of regions with high surface variability and the delineation of frontal masks using a dynamic threshold (90th percentile) of the distribution of gradient magnitudes $|\nabla V|$. In all products, the gradient distributions are strongly skewed, with a long tail toward high values, a typical feature of regions where fronts and discontinuities occupy a small fraction of the domain but concentrate most of the variability (see Table 2 and Figure 3).

As an example, the gradient magnitude fields across all variables exhibit strongly right-skewed probability density functions with prolonged tails representing localized, highly active structures. The background pelagic ocean is characterized by values close to zero, while specialized frontal zones reach extreme, physical values up to 3.20×10^{-4} °C/m for SST, 5.06×10^{-5} PSU/m for SSS, 5.56×10^{-4} $\log_{10}(\text{mg/m}^3)$/m for CHL, and 1.31×10^{-5} m/m for SSH. The frontal threshold was defined as the 90th percentile (P90) of the valid gradient magnitude values. These values were calculated independently for each variable and month, a decision motivated by the strongly right-skewed distribution of gradient magnitudes. This distribution reflects the fact that most of the domain is characterized by background waters with relatively low gradients, whereas localized frontal structures cor-

respond to the upper tail of the distribution. Consequently, the selected percentile provides a consistent criterion for identifying regions with the highest gradients while adapting the threshold to the specific magnitude and variability of each variable and month.

Table 2. Descriptive statistics of $|\nabla V|$.

Variable	Mean	P75	Maximun	Skewness
SST (°C/m)	1.45×10^{-5}	1.78×10^{-5}	3.20×10^{-4}	3.55
CHL ($\log_{10}$(mg/m^3)/m)	1.44×10^{-5}	1.69×10^{-5}	5.56×10^{-4}	4.93
SSH (m/m)	1.59×10^{-6}	2.11×10^{-6}	1.31×10^{-5}	1.83
SSS (PSU/m)	5.56×10^{-6}	7.33×10^{-6}	5.06×10^{-5}	–

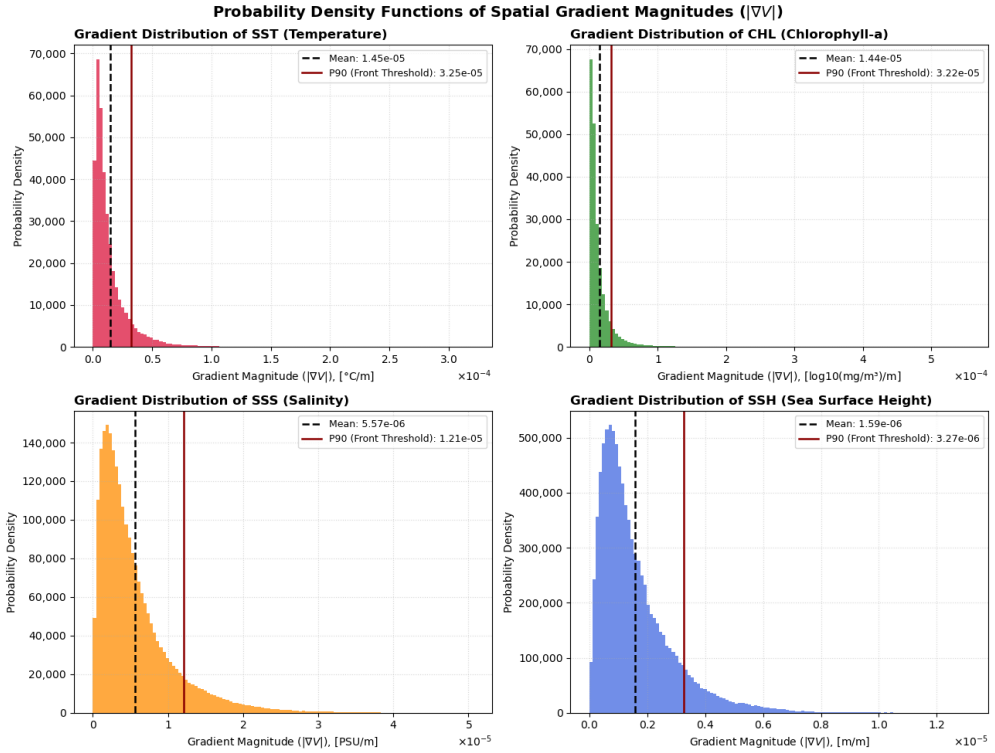


Figure 3. Probability Density Functions of Spatial Gradient Magnitudes.

To assess the effect of using a fixed rather than month-specific threshold, GRADHIST was compared with a global SST gradient threshold calculated from all valid gradient values for 2023. The global P90 was 3.25×10^{-5} °C/m, which was applied uniformly across all months. This fixed-threshold approach produced substantial seasonal differences in the detected frontal area, ranging from 0.58% in March to 20.78% in August, compared with the approximately 10% selected by the monthly P90 criterion. The spatial differences are illustrated for March and August in Figure 4, where we can observe how the fronts have been highlighted in yellow, while the remaining territory without fronts is shown in purple. In March, the global threshold identified substantially fewer frontal pixels than GRADHIST, whereas in August it identified a much larger area. These results demonstrate that a fixed threshold is strongly influenced by the seasonal variability of gradient magnitudes, whereas the month-specific P90 adapts the detection criterion to the distribution of gradients in each month.

Figure 5 shows the mosaics for March, July, and November illustrating the seasonal evolution of frontal activity. In March, coinciding with maximum thermal and biological gradients, the maps show a network of filaments and convergence zones around the Western Gyre and along the Almeria–Oran Front. In July, thermal frontal structures weaken

due to summer stratification, although SSH gradients continue to clearly delineate the semi-permanent gyres. In November, partial reactivation of fronts is observed in both SST and CHL, possibly linked to increased vertical mixing and destabilization of the surface layer.

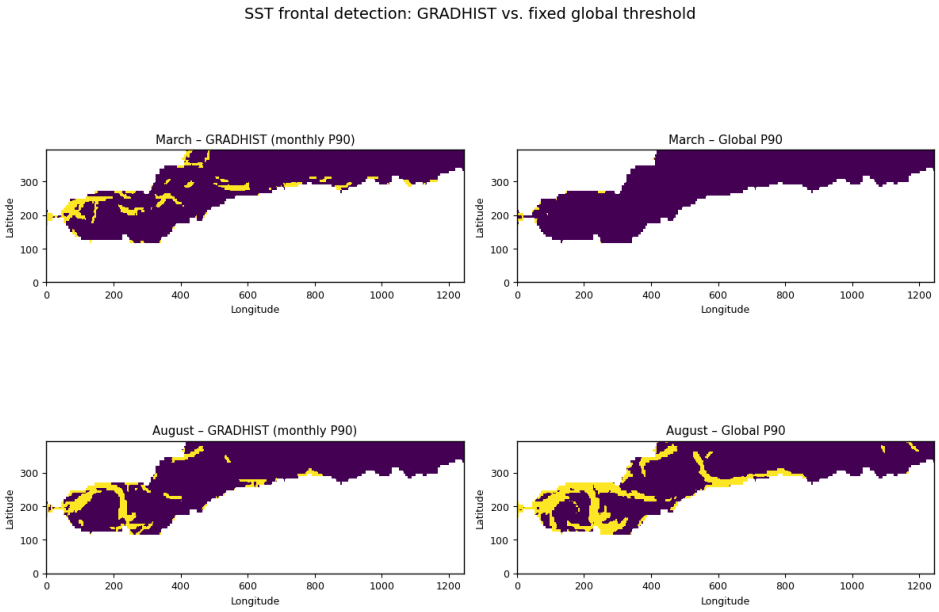


Figure 4. Comparison of SST frontal structures detected using GRADHIST with a month-specific P90 threshold and a fixed global P90 threshold for March and Auguste. Highlighted fronts (yellow) and front-free areas (purple).

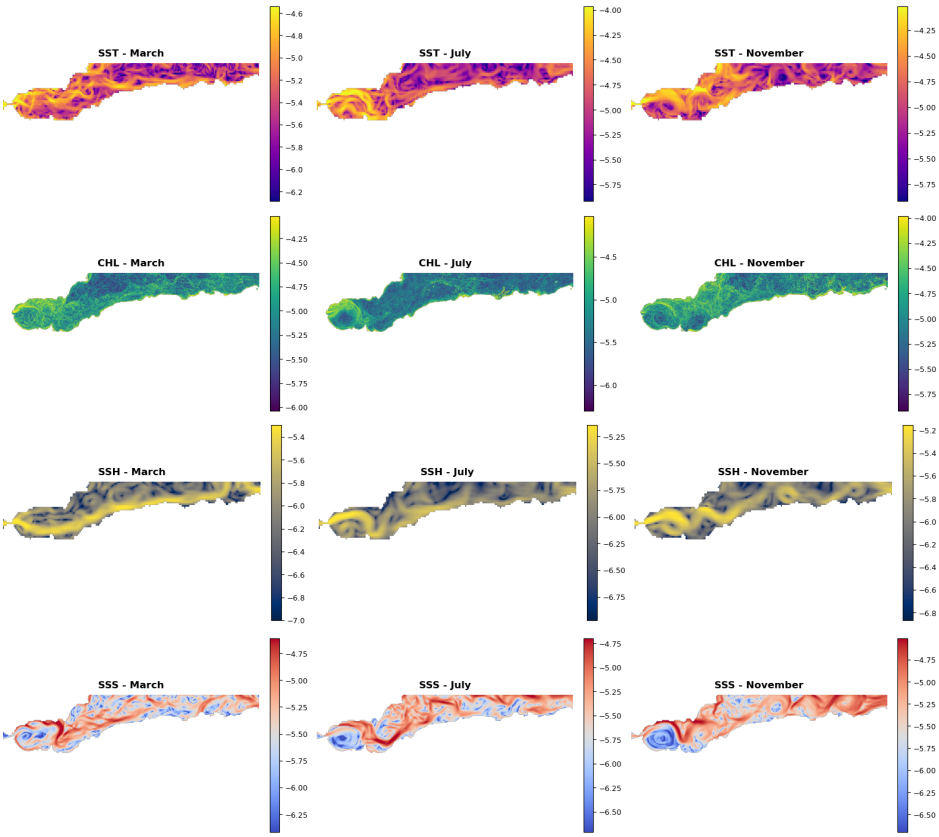


Figure 5. Evolution of the four variable horizontal gradient intensities in the Alboran Sea during 2023.

Monthly front counts (Figure 6) and intensity statistics (mean and maximum per front—see Table 3) show coherent seasonal patterns across variables, with important

differences depending on the physical or biological nature of each variable. In the case of sea surface temperature, monthly front numbers clearly increase during late winter and spring (March–May), reaching maximum values in both front count and mean intensity during this period.

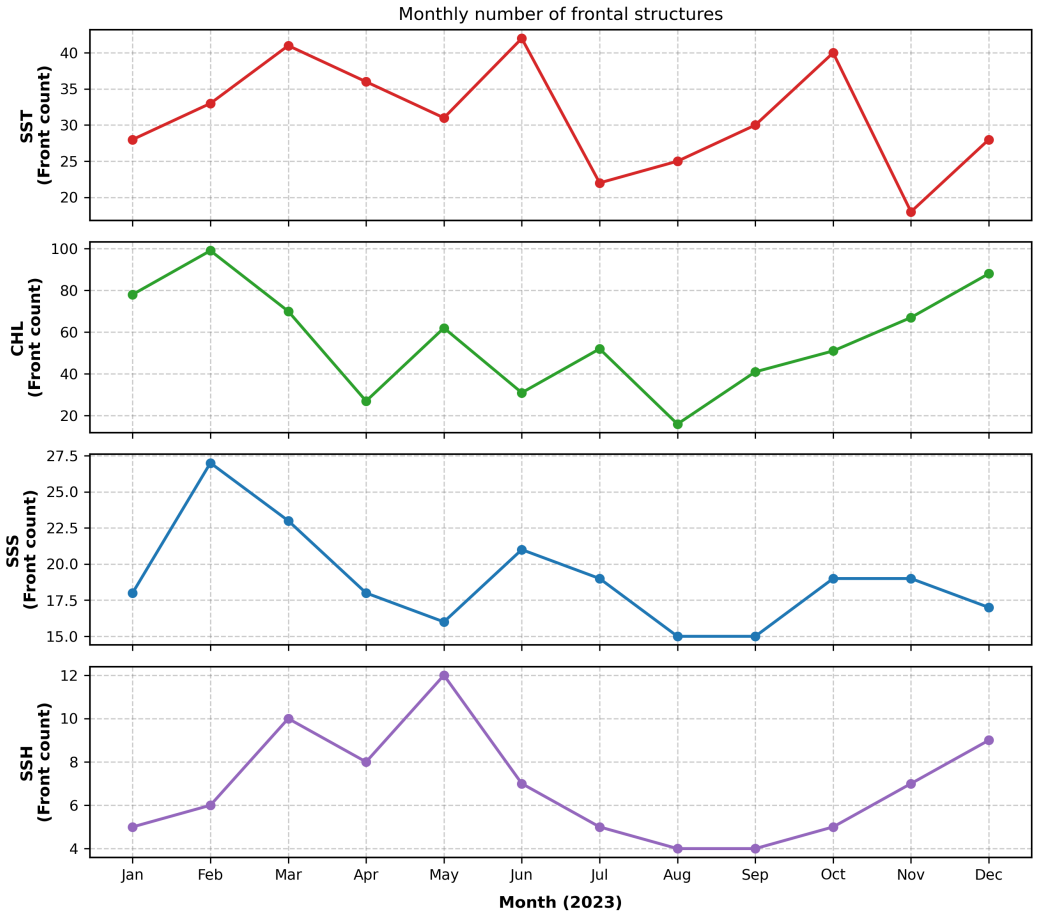


Figure 6. Monthly number of frontal structures.

Monthly front counts show lower seasonal variability, but SSS fronts clearly delineate the boundaries between Atlantic and Mediterranean waters, particularly along the central axis of the Alboran Sea and off the Almeria coast. Sea surface height behaves more independently, showing lower seasonal variability (in numerical terms), while zones of maximum intensity are consistently located around the semi-permanent gyres (Western and Eastern Alboran Gyres).

As shown in Figure 7, the temporal evolution of SST and CHL gradient intensities exhibits a distinct seasonal with contrasting periods of maximum frontal intensity rather than a persistent simultaneous peak. CHL gradient intensity presents its highest values during the cold period (late autumn to early spring, peaking above $2.0 \times 10^{-5}\,\log_{10}(\mathrm{mg \cdot m^{-3}})/\mathrm{m}$, followed by a sharp decline during the summer months (June–September) where values drop below $0.5 \times 10^{-5}\,\log_{10}(\mathrm{mg \cdot m^{-3}})/\mathrm{m}$. In contrast, SST gradient intensity increases progressively from spring into late summer, peaking in August (>2.3 $\times 10^{-5}\,^{\circ}\mathrm{C/m}$). A second synchronized peak appears in late autumn (November), where both SST and CHL gradients experience a rapid simultaneous intensification.

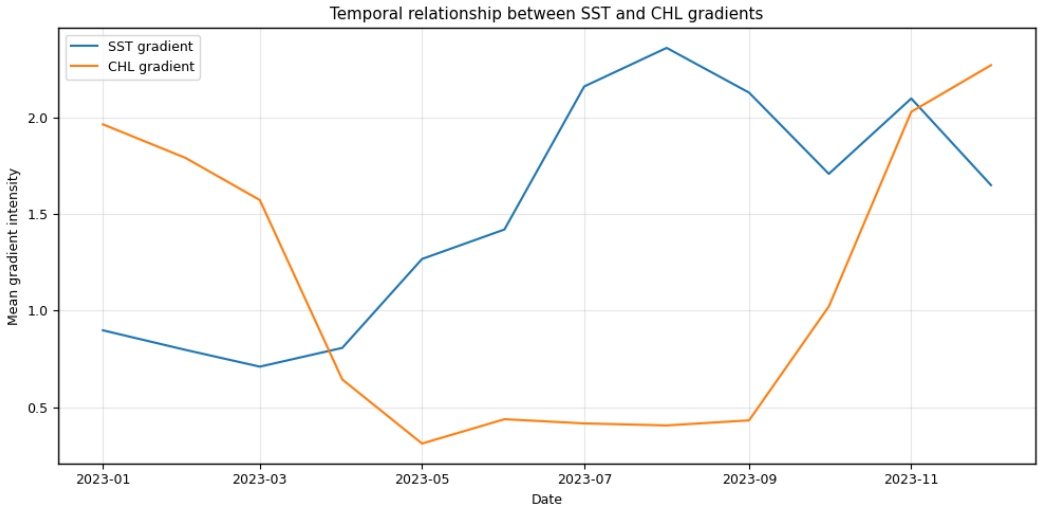


Figure 7. Relationship between SST and CHL gradients.

The temporal relationship between SST and CHL frontal gradients was further assessed using correlation analysis. The results showed a weak negative association between the two variables, with a Pearson correlation coefficient of $r = -0.313$ ($p = 0.322$) and a Spearman rank correlation coefficient of $\rho = -0.364$ ($p = 0.245$). Although the negative coefficients suggest an inverse tendency between SST and CHL frontal variability, the correlations were not statistically significant. This result indicates that the temporal variability of CHL frontal structures cannot be explained solely by the seasonal variability of SST, suggesting that additional physical and biological processes may contribute to the observed CHL frontal dynamics.

The accumulation of monthly frontal masks into density maps (frequency of frontal occurrence per pixel during 2023) highlights persistent zones of submesoscale activity. Across all products, at least three main hotspots can be identified (Figure 8).

- Western gyre (central Alboran region): High recurrence of fronts in SST, SSH, and CHL, consistent with water mass interactions and filament formation around the gyre. Persistent gradients in SST, SSH, and CHL are observed, associated with the interaction between Atlantic and Mediterranean waters and the recurrent presence of surface filaments.
- Almeria–Oran Front: Evident in SST, SSS, and CHL as a coastal-to-offshore band with high frontal frequency throughout the year. It appears in all variables, with particularly strong expression in SSS and SST, acting as a first-order physical and bio-geochemical boundary.
- North African shelf/souther domain margin: Fronts in this area are dominated by CHL and SSS, potentially linked to coastal upwelling and seasonal baroclinic instabilities.

Seasonal analysis of the density maps reveals a larger spatial extent and higher number of fronts in spring, a reduction during summer associated with thermal homogenization, and partial reactivation during autumn. Structures detected in SSH show remarkable spatial persistence, whereas those in CHL and SST are more transient, reinforcing the idea that submesoscale processes in the region are modulated both by background circulation and by the seasonality of atmospheric forcing and exchange through the Strait of Gibraltar.

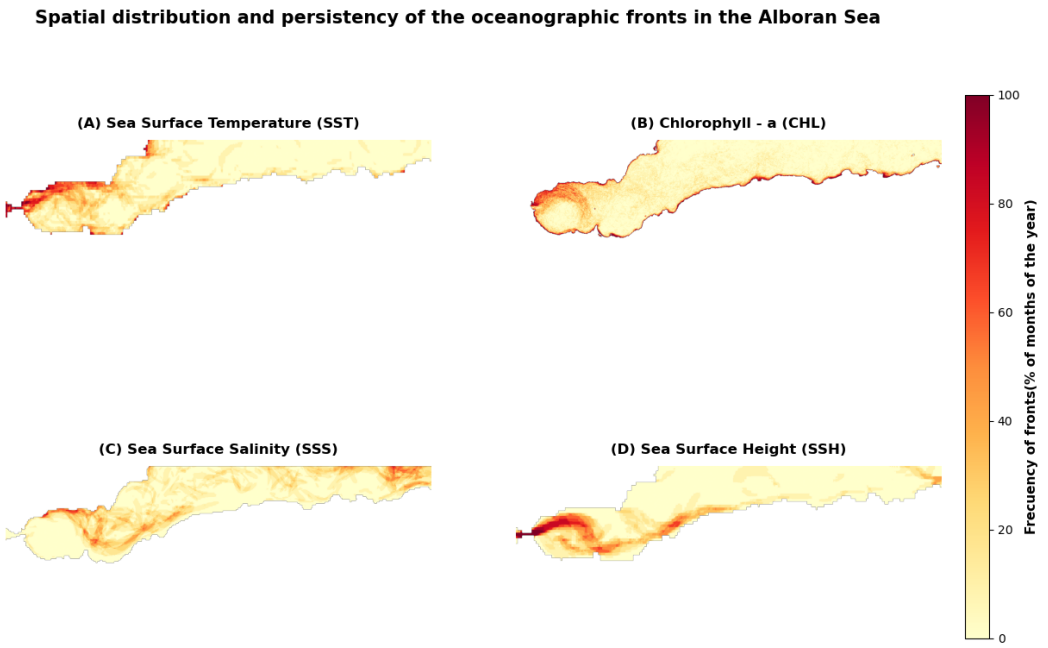


Figure 8. Spatial distribution of frontal density derived from SST, CHL, SSS, and SSH in the Alboran Sea during 2023.

Table 3. Mean and Maximum Intensity of gradients for CHL, SSH, SSS, and SST by quarter.

Quarter	Mean Intensity				Maximum Intensity			
	CHL	SSH	SSS	SST	CHL	SSH	SSS	SST
Q1 (January–March)	6.10×10^{-5}	4.20×10^{-6}	1.71×10^{-5}	2.52×10^{-5}	4.78×10^{-4}	1.06×10^{-5}	4.91×10^{-5}	1.14×10^{-4}
Q2 (April–June)	5.12×10^{-5}	4.42×10^{-6}	1.60×10^{-5}	3.94×10^{-5}	5.56×10^{-4}	9.55×10^{-6}	4.37×10^{-5}	3.20×10^{-4}
Q3 (July–September)	5.08×10^{-5}	4.53×10^{-6}	1.60×10^{-5}	7.48×10^{-5}	4.74×10^{-4}	1.05×10^{-5}	4.17×10^{-5}	2.65×10^{-4}
Q4 (October–December)	7.01×10^{-5}	4.83×10^{-6}	1.89×10^{-5}	5.48×10^{-5}	4.87×10^{-4}	1.31×10^{-5}	5.06×10^{-5}	1.73×10^{-4}

In Figure 9 we report the intensity of frontal gradients (specifically the maximum intensities reported in Table 3), it can be observed that the highest frontal activity for SST occurs during the second quarter (Q2: April–June), reaching maximum values on the order of $3.20 \times 10^{-4}\,^{\circ}\mathrm{C/m}$, whereas the maximum frontal gradient for SSS peaks during the fourth quarter (Q4: October–December) with a value of $5.06 \times 10^{-5}\,\mathrm{PSU/m}$. These values are consistent with typical submesoscale physical gradients in pelagic environments, successfully isolating the true dynamical structures (such as the Almeria-Oran front) from coastal boundaries.

For SSH, the mean frontal intensity remains low and remarkably stable throughout the year, fluctuating within a narrow range between 4.20×10^{-6} and $4.83 \times 10^{-6}\,\mathrm{m \cdot m^{-1}}$, which is consistent with the larger-scale geostrophic nature and smoother spatial gradients characteristic of sea surface height. Regarding CHL, its mean frontal intensity also operates on a subtle physical scale, ranging from 5.08×10^{-5} to 7.01×10^{-5} $\log_{10}(\mathrm{mg \cdot m^{-3}}) \cdot \mathrm{m^{-1}}$. The absence of a statistically significant correlation indicates that their temporal variability should not be interpreted as evidence of a direct SST–CHL coupling.

The temporal evolution of SST and CHL gradient intensities shows contrasting seasonal patterns: while CHL gradients generally increase during the colder months, SST gradients become more pronounced during warmer periods. However, the correlation analysis revealed only a weak negative association between the two variables, which was not statistically significant.

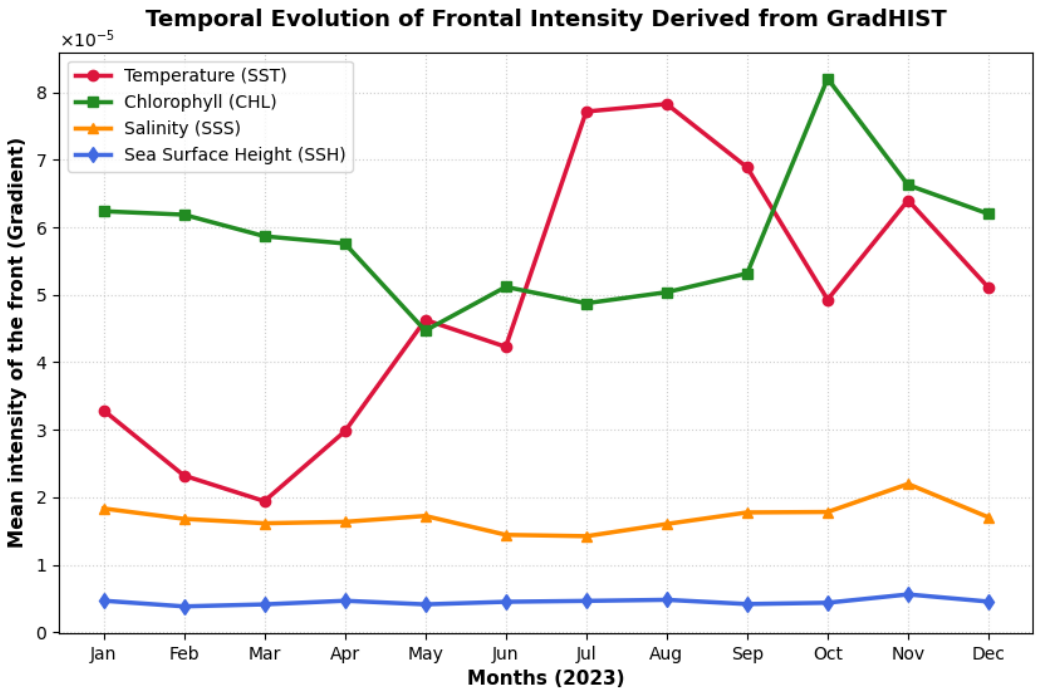


Figure 9. Temporal evolution of frontal intensity derived from SST, SSS, SSH, and CHL in the Alboran Sea during 2023.

5. Discussion

The temporal relationship between sea surface temperature (SST) and chlorophyll (CHL) gradient intensities (Figure 7) reveals a complex seasonal relationship between physical and biological frontal variability rather than a simple simultaneous spring peak. During winter and early spring, intense vertical mixing, surface cooling, and atmospheric forcing drive high biological productivity, resulting in pronounced CHL spatial gradients despite moderate surface thermal contrast. As summer approaches and solar irradiance intensifies, upper-layer thermal stratification reaches its maximum, driving SST gradient magnitudes to their annual peak while depleting surface nutrients and reducing CHL front intensity to minimum levels. This seasonal decoupling reflects the classic western Mediterranean transition between a light-limited, nutrient-rich winter regime and a stratified, nutrient-depleted summer regime. A simultaneous re-intensification of SST and CHL frontal structures is observed in late autumn, coinciding with atmospheric cooling and increased vertical mixing.

The comparison among variables highlights the multiscale nature of the system. Sea surface height (SSH) and sea surface salinity (SSS) exhibit lower intensities but high spatial persistence, indicating that they describe the background dynamic architecture dominated by semi-permanent gyres and Atlantic–Mediterranean exchange [4,17]. In contrast, SST and CHL show faster and more localized variability, linked to submesoscale frontal processes, lateral mixing, and coastal upwelling. This duality confirms that signals detected in SSH and SSS define the structural framework upon which short-term processes captured by SST and CHL are superimposed. The persistence of SSS fronts off Almeria and along the North African margin reinforces the role of the Atlantic–Mediterranean haline gradient as a stable component of surface circulation [5]. Gyre dynamics not only control temperature and salinity distributions but also modulate biomass dispersion and concentration, creating filaments and productivity patches that migrate seasonally. These observations are consistent with previous studies based on altimetry and numerical modeling that describe the Alboran gyres as semi-permanent structures modulated by atmospheric forcing and

Atlantic inflow [25,26]. From a bio-geochemical perspective, the co-occurrence of SST and CHL frontal variability highlights the role of fronts as zones of interaction between dynamics and biology. The coincidence of peaks in thermal and biological gradients during spring suggests that fronts act both as passive concentration mechanisms, accumulating laterally transported phytoplankton, and as zones of local enrichment where surface convergence and baroclinic instability can induce upwelling or vertical mixing [1,27]. These processes promote efficient redistribution of nutrients and biomass at scales of tens of kilometers, enhancing primary productivity in regions where external inputs are limited like in this Mediterranean oligotrophic waters.

From a methodological standpoint, the application of the GRADHIST algorithm enabled systematic, objective, and reproducible detection of fronts in multi-variable satellite fields. The use of a dynamic threshold based on percentiles adapted to the gradient distribution of each month and variable ensures method adaptability to different magnitudes and resolutions, reducing noise influence while preserving spatial coherence. The complementary spatial patterns detected across variables support the usefulness of the approach for multi-variable frontal characterization. Moreover, the combined use of physical and biogeochemical variables broadens system interpretation, allowing the joint interpretation of physical and biological frontal variability. The results position the GRADHIST method as a valuable tool for studying submesoscale dynamics and their ecological impact, broadening its initial application.

6. Conclusions

This study shows the ability of the GRADHIST algorithm to automatically and coherently identify frontal structures in the Alboran Sea using multi-variable satellite observations. Application of the method to sea surface temperature (SST), sea surface height (SSH), sea surface salinity (SSS), and chlorophyll-a (CHL) fields during 2023 enabled a detailed description of the spatial distribution and temporal evolution of fronts, revealing the hierarchical structure and physical–biological coupling that characterize the region. The results show a marked seasonality, with maximum front number and intensity occurring in the end of the winter season and early spring. This suggests that the temporal variability of biological frontal structures is influenced by multiple physical and biological processes rather than by SST variability alone. SSH and SSS, in contrast, define the background dynamic architecture, delineating semi-permanent gyres and the Almeria–Oran Front, which emerge as persistent structures throughout the year. The method proved robust and adaptable thanks to the use of a dynamic threshold that optimizes front detection across fields of different nature and dynamic range. The spatial and temporal patterns identified across the four variables provide complementary information on the frontal dynamics of the Alboran Sea.

The use of data cubes has been fundamental, as it significantly facilitated the processing and analysis of the four oceanographic variables over time. Organizing the data this way allowed for a more efficient and structured comparison of the frontal activity. This work lays the foundation for extending the use of the GRADHIST method to long-term time series and open the study area to adjacent regions, with the aim of assessing inter-annual variability, climatic trends, and the contribution of fronts to matter and energy fluxes in the Mediterranean.

Looking ahead, the products and data generated by this methodology could be very useful as inputs for ocean prediction and forecasting models, which is a direction we want to explore in our next studies. At the same time, we think it would be very valuable to test this approach using data with higher spatial resolution, such as 1 km products. Increasing the resolution would allow us to capture the finer details of submesoscale processes and

small filaments that are harder to identify with the current data, giving us a much more precise view of the frontal activity in the region.

Further validation using independent observations would be valuable to assess the robustness of the detected frontal structures beyond the internal consistency provided by the multi-variable analysis and the fixed-threshold baseline comparison.

Author Contributions: Conceptualization, A.B.R.; methodology, A.B.R.; software, E.M.-M.; formal analysis, E.M.-M. and A.B.R.; data curation, E.M.-M.; writing—original draft preparation, E.M.-M.; writing—review and editing, A.B.R.; supervision, A.B.R.; project administration, A.B.R.; funding acquisition, A.B.R. All authors have read and agreed to the published version of the manuscript.

Funding: This research received support from the European Space Agency Network of Resources Initiative and the DeepESDL project ID BIOTERMOFRONT.

Data Availability Statement: In preparation: Data cubes and Python 3.14 scripts will be available from Zenodo and Github as well as from the EarthCode project: https://earthcode.esa.int (accessed on 16 August 2026).

Acknowledgments: We acknowledge the support given by Brockmann Consult GmbH and the DeepESDL team. During the preparation of this manuscript/study, the author(s) used Gemini 3 Flash for the purposes of helping with the coding and improving the writing. We also used it for bibliographic research. The authors have reviewed and edited the output and take full responsibility for the content of this publication.

Conflicts of Interest: The authors declare no conflicts of interest.

References

1. Mahadevan, A. The impact of submesoscale physics on primary productivity of plankton. *Annu. Rev. Mar. Sci.* **2016**, *8*, 161–184. [CrossRef] [PubMed]
2. Pujol, M.-I.; Faugère, Y.; Taburet, G.; Dupuy, S.; Pelloquin, C.; Ablain, M.; Picot, N. DUACS DT2014: The new multi-mission altimeter data set reprocessed over 20 years. *Ocean Sci.* **2016**, *12*, 1067–1090. [CrossRef]
3. Marrec, P.; McNair, H.; Franzè, G.; Morison, F.; Strock, J.P.; Menden-Deuer, S. Seasonal variability in planktonic food web structure and function of the Northeast U.S. Shelf. *Limnol. Oceanogr.* **2021**, *66*, 1440–1458. [CrossRef]
4. Violette, P.E.L. The Advection of Submesoscale Thermal Features in the Alboran Sea Gyre. *J. Phys. Oceanogr.* **1984**, *14*, 550–565. [CrossRef]
5. Macias, D.; Garcia-Gorriz, E.; Stips, A. The seasonal cycle of the Atlantic Jet dynamics in the Alboran Sea: Direct atmospheric forcing versus Mediterranean thermohaline circulation. *Ocean. Dyn.* **2016**, *66*, 137–151. [CrossRef]
6. Vargas-Yáñez, M.; Moya, F.; García-Martínez, M.C.; Tel, E.; Zunino, P.; Plaza, F.; Salat, J.; Pascual, J.; López-Jurado, J.L.; Serra, M. Climate change in the Western Mediterranean sea 1900–2008. *J. Mar. Syst.* **2010**, *82*, 171–176. [CrossRef]
7. Sánchez-Garrido, J.C.; Lafuente, J.G.; Fanjul, E.Á.; Sotillo, M.G.; de los Santos, F.J. What does cause the collapse of the Western Alboran Gyre? Results of an operational ocean model. *Prog. Oceanogr.* ***2013***, 116, *142–153*; . [CrossRef]
8. Belkin, I.M.; Cornillon, P.C.; Sherman, K. Fronts in large marine ecosystems. *Prog. Oceanogr.* **2009**, *81*, 223–236. [CrossRef]
9. Bakun, A. Fronts and eddies as key structures in the habitat of marine fish larvae: Opportunity, adaptive response and competitive advantage. *Sci. Mar.* **2006**, *70*, 105–122. [CrossRef]
10. Nieto, K.; Demarcq, H.; McClatchie, S. Mesoscale frontal structures in the Canary Upwelling System: New front and filament detection algorithms applied to spatial and temporal patterns. *Remote Sens. Environ.* **2012**, *123*, 339–346. [CrossRef]
11. Kahru, M.; Di Lorenzo, E.; Manzano-Sarabia, M.; Mitchell, B.G. Spatial and temporal statistics of sea surface temperature and chlorophyll fronts in the California Current. *J. Plankton Res.* **2012**, *34*, 749–760. [CrossRef]
12. Lima, M.J.; Sala, I.; Caldeira, R.M.A. Physical Connectivity Between the NE Atlantic Seamounts. *Front. Mar. Sci.* **2020**, *7*, 238. [CrossRef]
13. Vázquez-Cuervo, J.; Font, J.; Martínez-Benjamin, J.J. Observations on the circulation in the Alboran Sea using ERS-1 altimetry and sea surface temperature data. *J. Phys. Oceanogr.* **1996**, *26*, 1426–1439. [CrossRef]
14. Kirches, G.; Paperin, M.; Klein, H.; Brockmann, C.; Stelzer, K. GRADHIST—A method for detection and analysis of oceanic fronts from remote sensing data. *Remote Sens. Environ.* **2016**, *181*, 264–280. [CrossRef]
15. Le Traon, P.Y.; Reppucci, A.; Alvarez Fanjul, E.; Aouf, L.; Behrens, A.; Belmonte, M.; Bentamy, A.; Bertino, L.; Brando, V.E.; Kreiner, M.B.; et al. From observation to information and users: The Copernicus Marine Service perspective. *Front. Mar. Sci.* **2019**, *6*, 234. [CrossRef]
16. von Schuckmann, K.; Le Traon, P.Y.; Smith, N.; Pascual, A.; Djavidnia, S.; Gattuso, J.P.; Grégoire, M.; Aaboe, S.; Alari, V.; Alexander, B.E.; et al. Copernicus Marine Service Ocean State Report, Issue 5. *J. Oper. Oceanogr.* **2021**, *14*, 1–185. [CrossRef]

17. Vargas-Yáñez, M.; Plaza, F.; Garcıa-Lafuente, J.; Sarhan, T.; Vargas, J.; Vélez-Belchí, P. About the seasonal variability of the Alboran Sea circulation. *J. Mar. Syst.* **2002**, *35*, 229–248. [CrossRef]
18. Vargas-Yáñez, M.; Ramírez, T.; Cortés, D.; Sebastián, M.; Plaza, F. Warming trends in the continental shelf of Málaga Bay (Alborán Sea). *Geophys. Res. Lett.* **2002**, *29*, 39-1–39-4. [CrossRef]
19. Heburn, G.W.; La Violette, P.E. Variations in the structure of the anticyclonic gyres found in the Alboran Sea. *J. Geophys. Res. Ocean.* **1990**, *95*, 1599–1613. [CrossRef]
20. Viúdez, A.; Pinot, J.M.; Haney, R. On the upper layer circulation in the Alboran Sea. *J. Geophys. Res. Ocean.* **1998**, *103*, 21653–21666. [CrossRef]
21. Ruiz, J.; Echevarrıa, F.; Font, J.; Ruiz, S.; Garcıa, E.; Blanco, J.; Jiménez-Gómez, F.; Prieto, L.; González-Alaminos, A.; Garcıa, C.; et al. Surface distribution of chlorophyll, particles and gelbstoff in the Atlantic jet of the Alborán Sea: From submesoscale to subinertial scales of variability. *J. Mar. Syst.* **2001**, *29*, 277–292. [CrossRef]
22. Millot, C. Circulation in the western Mediterranean Sea. *J. Mar. Syst.* **1999**, *20*, 423–442. [CrossRef]
23. Canny, J. A computational approach to edge detection. *IEEE Trans. Pattern Anal. Mach. Intell.* **1986**, *8*, 679–698. [CrossRef]
24. Cayula, J.F.; Cornillon, P. Edge detection algorithm for SST images. *J. Atmos. Ocean. Technol.* **1992**, *9*, 67–80. [CrossRef]
25. Pascual, A.; Ruiz, S.; Olita, A.; Troupin, C.; Claret, M.; Casas, B.; Mourre, B.; Poulain, P.M.; Tovar-Sanchez, A.; Capet, A.; et al. A multiplatform experiment to unravel meso-and submesoscale processes in an intense front (AlborEx). *Front. Mar. Sci.* **2017**, *4*, 39. [CrossRef]
26. Troupin, C.; Pascual, A.; Ruiz, S.; Olita, A.; Casas, B.; Margirier, F.; Poulain, P.M.; Notarstefano, G.; Torner, M.; Fernández, J.G.; et al. The AlborEX dataset: Sampling of sub-mesoscale features in the Alboran Sea. *Earth Syst. Sci. Data* **2019**, *11*, 129–145. [CrossRef]
27. Lévy, M.; Ferrari, R.; Franks, P.J.; Martin, A.P.; Rivière, P. Bringing physics to life at the submesoscale. *Geophys. Res. Lett.* **2012**, *39*, L14602. [CrossRef]

Disclaimer/Publisher's Note: The statements, opinions and data contained in all publications are solely those of the individual author(s) and contributor(s) and not of MDPI and/or the editor(s). MDPI and/or the editor(s) disclaim responsibility for any injury to people or property resulting from any ideas, methods, instructions or products referred to in the content.